J Mater Sci (2010) 45:2181–2187
DOI 10.1007/s10853-009-3951-4

HTC2009

Direct bonding of Cu to oxidized silicon nitride by wetting of molten Cu and Cu(O)

Shun-Ichiro Tanaka

Received: 15 June 2009 / Accepted: 3 October 2009 / Published online: 31 October 2009
© Springer Science+Business Media, LLC 2009

Abstract When pressureless sintered silicon nitride with the main additives Y_2O_3 and Al_2O_3, having a thermal conductivity $K = 20$ W/m K, was oxidized at 1240–1360 °C in still air, the resulting surface oxide layer easily bonded to a copper plate in the temperature region between 1065 and 1083 °C, and in the oxygen concentration range of 0.008–0.39 wt%, as shown in a Cu–O phase diagram. The oxide on the silicon nitride was characterized as $Y_2O_3{\cdot}2SiO_2$ and mixed silicate glass with additives and impurities that diffused through the grain boundary. The bonding strength of Cu/Si_3N_4 depends on the amount or layer thickness of silicate glass and reaches as high as 100 MPa by shear at room temperature. Detailed analysis of the oxidation layer and the peeled-off surfaces of directly bonded Si_3N_4/Cu reveal that the main mechanism of bonding is wetting to glassy silicate phase by mixtures of molten Cu and α-solid solution Cu(O), which solidify to $\alpha + Cu_2O$ below 1065 °C by a eutectic reaction. The direct reactive wetting of molten Cu, supplied from the grain boundary of a Cu plate, on the glassy phase enables very tight chemical bonding via oxygen atoms.

Introduction

One of the key factors for the wide application of engineering ceramics is bonding technologies to metals for which metallization and active metal brazing have been developed for oxide and non-oxide ceramics. It is necessary to develop technologies for relaxing residual stresses between ceramics and metals for higher bonding strength. Considering both materials properties and industrial mass productivity, it is also necessary to develop bonding technologies for low-temperature, pressureless processes, and for complicated shapes.

The bonding method using the Cu–O hypo-eutectic reaction has been well-known as 'direct bond copper (DBC)', which was first developed by Burgess et al. [1] for oxide ceramics, and this method has been widely used to bond a Cu plate with Al_2O_3 [2–4] and oxidized AlN plates having a thermal conductivity $K = 120$ W/m K as a heat dissipative substrate for power transistors [5]. The first successful direct bonding of Cu to oxidized Si_3N_4 with the main additives Y_2O_3 and Al_2O_3 was reported by the author in 1983 [6] when he realized automotive engine components for which a pressureless sintered Si_3N_4, which is suitable for components having complicated shapes, was used. In 1990, Kim et al. [7] also succeeded to bond Cu to Si_3N_4 with MgO additive, but weak bond 10 MPa was reported. These Si_3N_4 had a low K of 20 W/m K, but long-term technological development has led to substrates with K higher than 70 W/m K and with peel strength and fatigue life greater than those of Al_2O_3 and AlN plates.

In this paper, I aim to reveal the characteristics of a directly bondable surface/interface of oxidized Si_3N_4 related to the "direct bonding" method, which will be potentially useful bonding method for heat-dissipative substrates. Extensive and accumulated studies on the characterization of the Cu-bondable oxidation products on Si_3N_4 and the Si_3N_4/Cu interface are reported and the bonding mechanism is discussed.

S.-I. Tanaka (✉)
Institute of Multidisciplinary Research for Advanced Materials, Tohoku University, 2-1-1, Katahira, Aoba-ku, Sendai 980-8577, Japan
e-mail: sitanaka@tagen.tohoku.ac.jp

Experimental

The ceramic specimens used in this study were made of pressureless sintered β-silicon nitride, TSN-03, supplied by Toshiba Corporation including a few metallic impurities such as Ca, Mg, and Fe. 4.4 wt% Y_2O_3, 3.5 wt% Al_2O_3, and others were added as sintering agents. They had a thermal conductivity $K = 20$ W/m K and a 4-point bending strength $\sigma_{4B} = 950$ MPa between room temperature and 1000 °C. The Si_3N_4 specimens used had dimensions of about 25 × 15 × 5 mm^3 for the oxidation and bonding experiments and were pretreated and oxidized at 1200–1415 °C for 10.4 h (3.74 × 10^4 s) on an Al_2O_3–SiO_2 substrate in still air.

Oxidation characteristics were analyzed by determining weight gain based on the conditions for diffusion-controlled processes to compare activation energies. Oxidation products on Si_3N_4 ceramics were characterized by X-ray diffraction (XRD) analysis, optical microscopy (OM), scanning electron microscopy with energy dispersive X-ray analysis (SEM–EDX), and electron probe microanalysis (EPMA).

The metal specimen bonded to Si_3N_4 was a tough-pitch copper plate 0.3 mm thick containing 0.02–0.05 wt% oxygen as Cu_2O. The bonding of oxidized Si_3N_4 to copper was held without pressure between 1075 and 1080 °C for 10 min in inert gas to induce a hypo-eutectic reaction in the Cu–O system. Cross-sectional views of the joint were observed by SEM and EPMA.

Bonding strength was measured and compared by applying shear at room temperature in the Si_3N_4/Cu/Si_3N_4 joint at a cross-head speed of 1 mm/min. Peeled-off surfaces on Si_3N_4 and Cu were also observed by SEM and EPMA.

Results and discussion

Oxidation characteristics and kinetics of pressureless sintered Si_3N_4

A plot of weight gain Δw by the oxidation of pressureless sintered Si_3N_4 with additives of Y_2O_3 and Al_2O_3 at 1200–1415 °C for 10.4 h is shown in Fig. 1. The oxidation resistance of pressureless sintered Si_3N_4 is lower than that of hot-pressed or hot-isostatic-pressed Si_3N_4 because of the large amount of additives. The change in weight gain in this research apparently shows two regions, that is, 1200–1315 °C and 1315–1415 °C, but the change in Δw can be labeled Regions I, II, and III taking into account the kinetics analyzed in Fig. 2.

If the oxidation of materials is a diffusion-controlled process, the weight gain Δw obeys the parabolic law versus oxidation time t and is written as Eq. 1 using the rate constant K, the activation energy Q, and the gas constant R. When the oxidation temperature T is changed under a constant oxidation time, the activation energy of the oxidation can be obtained from the Arrhenius plot of Eq. 2.

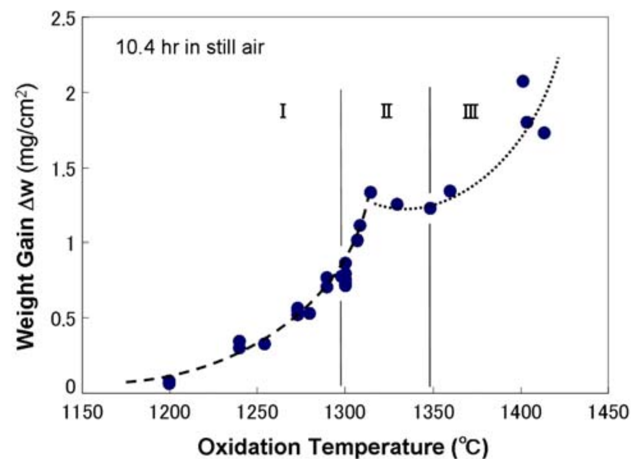

Fig. 1 Weight gain of pressureless sintered silicon nitride with main additives of Y_2O_3 and Al_2O_3 by oxidation at 1200–1415 °C for 10.4 h in still air. The change in weight gain apparently shows two stages, as shown by *dotted lines*, but the change in weight gain can be divided into Regions I, II, and III on the basis of oxidation kinetics and surface morphology observation

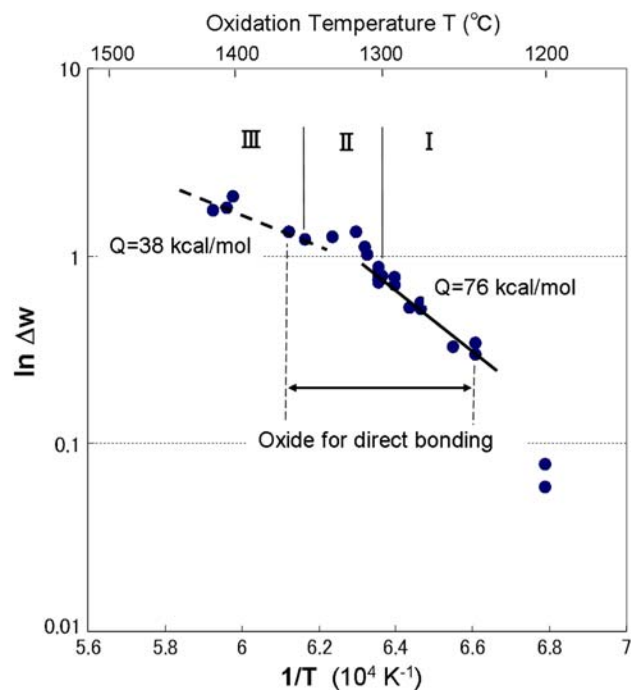

Fig. 2 Arrhenius plot for oxidation weight gain Δw of pressureless sintered Si_3N_4 shown in Fig. 1. The oxidation was found to be diffusion-controlled process and divided into three stages: Regions I, II, and III. Oxides that may undergo to direct bonding to Cu existed in Regions I and II

$$\Delta w = t^{1/2} \cdot K = t^{1/2} \cdot K_0 \exp(-Q/RT) \qquad (1)$$

$$\ln \Delta w = \ln K_0' - Q/RT \qquad (2)$$

The oxidation weight gain Δw of pressureless sintered Si_3N_4 in this study obeyed the parabolic law at 1300 °C, and the Δw–T relation shown in Fig. 1 can be plotted in Arrhenius-type Eq. 2, as shown in Fig. 2. Two straight lines mean diffusion-controlled process in the oxidation of Si_3N_4 and the change in Δw was divided into three stages: Region I with activation energy $Q = 76$ kcal/mol (3.3 eV) at 1240–1300 °C, Region II a transition region, and Region III with $Q = 38$ kcal/mol (1.7 eV) at 1350–1415 °C. Oxides capable of direct bonding to Cu existed in Regions I and II, as discussed in "Shear strength of directly bonded Si_3N_4/Cu" section.

The diffusion process and diffusant can be discussed from the two activation energies. $Q = 38$ kcal in Region III roughly matches that of silicon dioxide formation, $Q = 45$ kcal/mol; on the other hand, $Q = 76$ kcal/mol in Region I is higher and does not match with any activation energy reported in the literature. The higher activation energy is supposed to be that of the grain boundary diffusion of additives such as Y and Al or impurities such as Ca and Mg contained in hot-pressed sintered Si_3N_4 [8].

Surface morphology and phases in oxidized Si_3N_4

The surface morphologies of 10.4-h-oxidized pressureless sintered Si_3N_4 were observed by OM and SEM, and the results are shown in Fig. 3 relating to the plot of weight gain versus temperature (Fig. 1). The main morphologies of the surface oxide were flaky precipitates in Region I, a glassy phase in Region II, and needlelike precipitates in Region III. Two typical XRD patterns of the oxide formed on pressureless sintered β-Si_3N_4 were obtained, as shown in Fig. 4. $Y_2O_3 \cdot 2SiO_2$ (Y2S) and cristobalite existed on the surface as a crystal phase and the amount of glassy phase as a background increased in the Cu Kα diffraction profile at around $2\theta = 15°$–$35°$. A small amount of unknown phase also exists. The peak intensity of Y2S and the amount of the characteristic glassy phase measured from an area of the background for each oxidation temperature are shown in Fig. 5 in which Regions I–III, labeled in Fig. 2, are marked in the upper vertical axis.

The characteristics of the oxidation products are summarized taking account of the morphology and XRD results shown in Figs. 3, 4, and 5: Extraordinarily high (110), (220), and (330) diffraction peaks of Y2S in Region I suggest platelike Y2S crystals 20 µm in length arrayed with their (110) plane parallel to the Si_3N_4 substrate interface. A large amount of glassy phase in Region II indicates that Y2S crystals distributed nearly randomly in the thick glass layer, showing that the standard highest diffraction peak of Y2S (021) was observed. α-Cristobalite was detected in all regions but its amount increased largely in Region III, showing a needlelike crystal in Fig. 3 accompanied by preferred-oriented Y2S in the oxide layer where both have a very rugged surface and show difficulty in chemical tight bonding to metals without pressure.

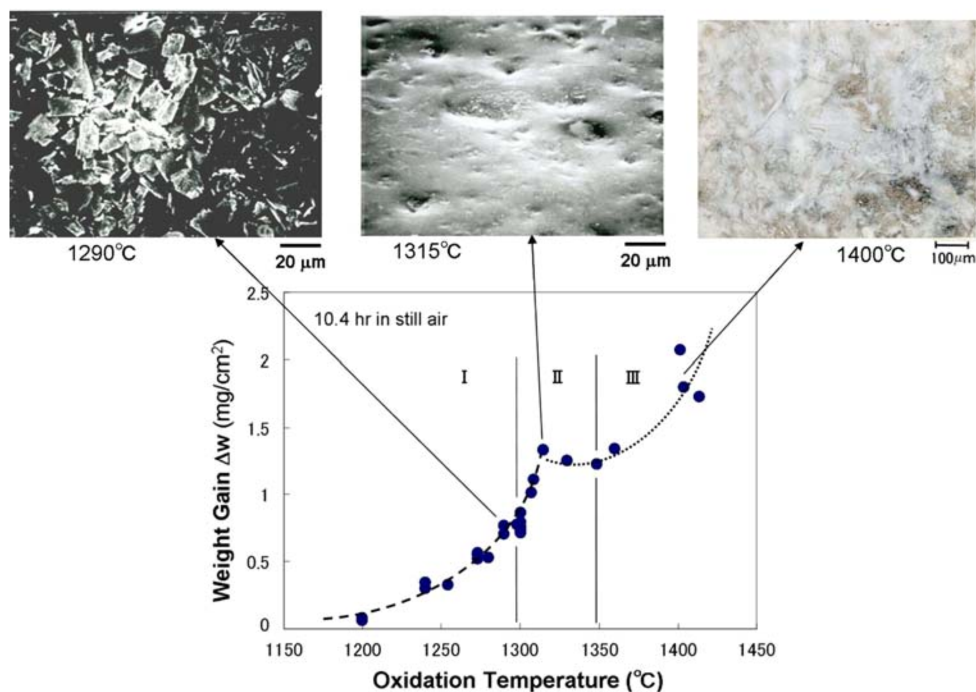

Fig. 3 Surface morphologies of oxidized pressureless sintered Si_3N_4. Characteristics of the surface oxides were flaky precipitates in Region I, a glassy phase in Region II, and needlelike precipitates in Region III

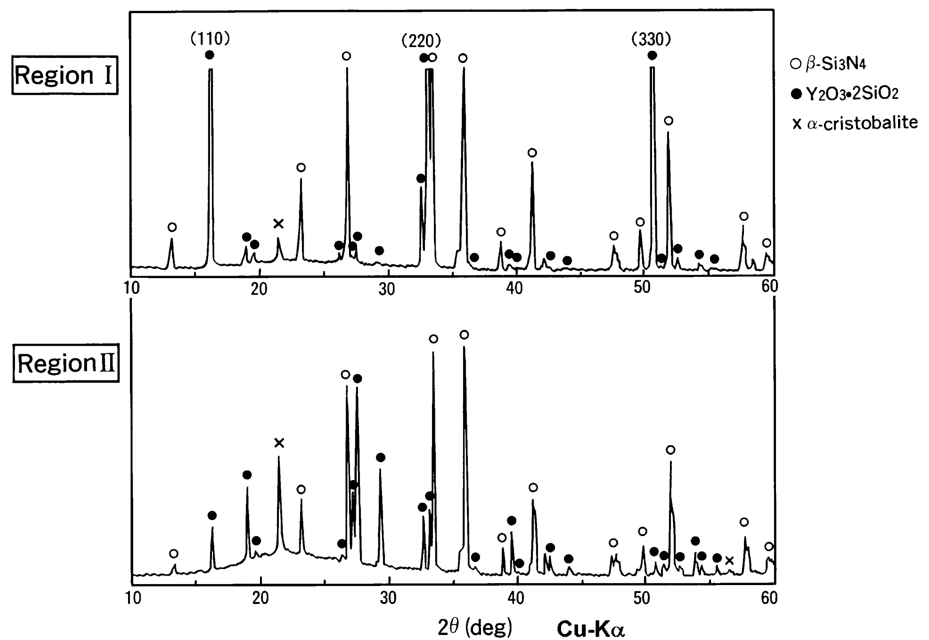

Fig. 4 Typical X-ray diffraction patterns of the oxides formed on pressureless sintered Si_3N_4. $Y_2O_3{\cdot}2SiO_2$ (Y2S) and cristobalite exist on the surface as a crystal phase and a glassy phase, respectively, accompanied by as a background increase in the Cu Kα diffraction profile at around $2\theta = 15°–35°$

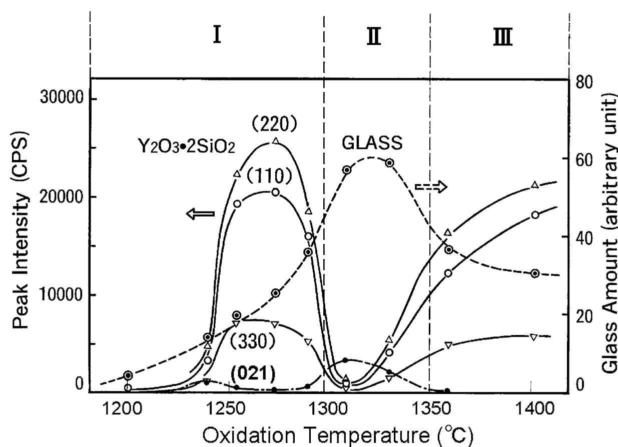

Fig. 5 Changes in peak intensity of $Y_2O_3{\cdot}2SiO_2$ (Y2S) and glass amount with oxidation temperature for pressureless sintered Si_3N_4 after oxidation for 10.4 h. Y2S crystallized with its (110) plane parallel to the Si_3N_4 surface in Region I, whereas Y2S randomly distributed inside a large amount of glass phase in Region II

The abrupt and discontinuous increase in the weight gain Δw in Region II shown in Fig. 1 can be explained by the formation of a thick layer of glass. Y2S crystals seem to precipitate from the glass phase, which involves mixed silicates containing oxides of concentrated impurities. The existence of these phases reported in Si_3N_4–Y_2O_3–Al_2O_3 oxidation [9] and Y2S formation is reasonable considering the phase diagram of the Si_3N_4–SiO_2–Y_2O_3 system [10]. The small pores observed in the glassy phase may be caused by N_2 gas, which evolved during oxidation [7, 11].

Shear strength of directly bonded Si_3N_4/Cu

Pressureless sintered Si_3N_4 oxidized for 10.4 h bonded directly to a tough-pitch copper plate by a Cu–O hypo-eutectic reaction to form a sandwich-type Si_3N_4/Cu/Si_3N_4 joint. Bonding strength was measured by shearing at room temperature. The shear strength of the joint changed drastically with the oxidation temperature of Si_3N_4, as shown in Fig. 6. Successful bonding was observed in the

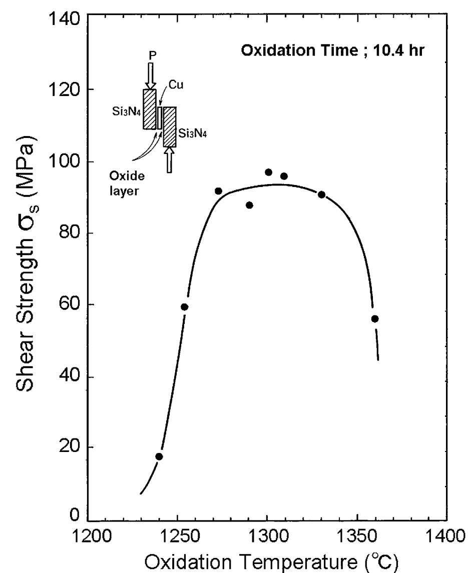

Fig. 6 Shear strength of the Si_3N_4/Cu/Si_3N_4 joint directly bonded by Cu–O hypo-eutectic reaction related to the oxidation temperature of Si_3N_4. The bonding strength is as high as 90–100 MPa in the temperature range of 1270–1330 °C corresponding to Region I and the tail of Region II

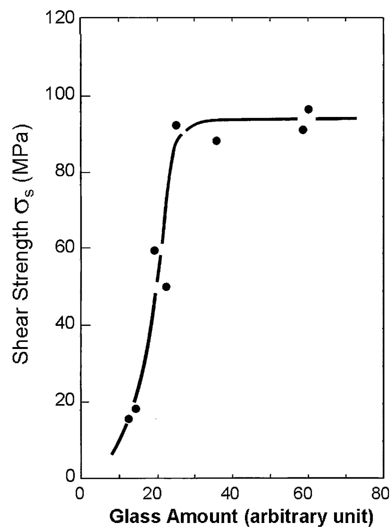

Fig. 7 Bond strength of the joint related to glass amount in the oxidation products measured from XRD profiles. It exhibits saturation at 90–100 MPa

oxidation temperature range of 1240–1360 °C in Regions I–II in Figs. 1, 3, and 5. No successful bonding was observed at oxidation temperatures of 1200 and 1400 °C. Bonding strength reached as high as 90–100 MPa in the temperature range of 1270–1330 °C, which corresponded to Region I and the tail of Region II.

The trend of bonding strength was compared with those of the morphology and phases, as shown in Figs. 3 and 5, to discuss the role of the glassy phase in the oxide layer. Bonding strength closely correlates to glass amount, rewritten as Fig. 7 from Figs. 5 and 6, rather than to the presence of the Y2S plate, and it increases with glass amount and saturates. The glass amount evaluated from the XRD profile can be converted using the factor 0.012 mm^3/unit obtained by checking the cross-sectional image, such as that in Fig. 8. The relation of bonding strength to glass amount implies that the bonding strength of the joint was determined by the fracture strength of the glassy phase in the oxide layer. Comparing with the tensile strength 10 MPa in Si_3N_4/Cu joint reported by Kim et al. [7] who used MgO as a sintering additive, a different crystal phase $MgSiO_3$ formed without glassy phase.

Interface structures of bonded Si_3N_4/Cu

Cu with a small amount of oxygen dissolved reacted well with the oxide on Si_3N_4 to form directly bonded couples. Cross-sectional views of the joined interface and peeled-off surfaces of Si_3N_4 and Cu were observed by SEM and EPMA, which led to the suggestion of a bonding mechanism.

Figure 8 shows a SEM cross-sectional view of the bonded Si_3N_4/Cu and the element distribution around the interface as analyzed by EPMA. Since Si_3N_4 was oxidized at 1300 °C for 10.4 h, Y2S crystals distributed randomly in the thick glass layer, about 6.6 μm in thickness, which is characteristic of Region II. Y, Al, and Ca atoms condensed in the oxide layer, forming Y2S and silicate glass. They diffused out during oxidation by grain boundary diffusion to the surface for Y and Al atoms from the sintering additives, namely, Y_2O_3 and Al_2O_3, and for Ca from inevitable impurities in the raw materials of α-Si_3N_4 powder. Spectroscopic analysis also revealed the presence of Mg and Fe atoms other than Ca atoms as reported in the literature [8, 9]. The glass layer seems to be composed of a mixture of SiO_2–CaO–MgO–Fe_2O_3–Al_2O_3–other oxide.

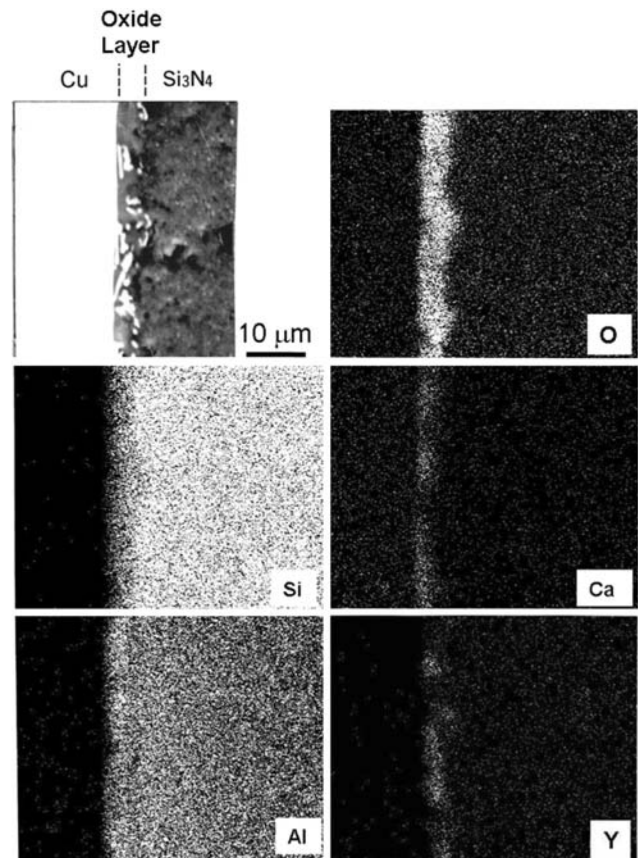

Fig. 8 SEM cross-sectional view and the element distribution around the interface analyzed by EPMA of bonded Cu to Si_3N_4, which is oxidized at 1300 °C for 10.4 h. Y, Al, and Ca atoms diffused out and condensed into the oxide layer forming Y2S and silicate glass. Y2S crystals distributed randomly in the thick glass layer characteristic of Region II

The oxide layer in Region II enables Cu to bond Si_3N_4 tightly. It is observed that there is a continuous interface between oxides and Cu, and peeled fracture occurs just in oxidation products. Figure 9 shows the peeled-off surfaces of Cu and Si_3N_4 oxidized at 1300 °C for 10.4 h and both sides have a glassy phase like adhesives accompanied by

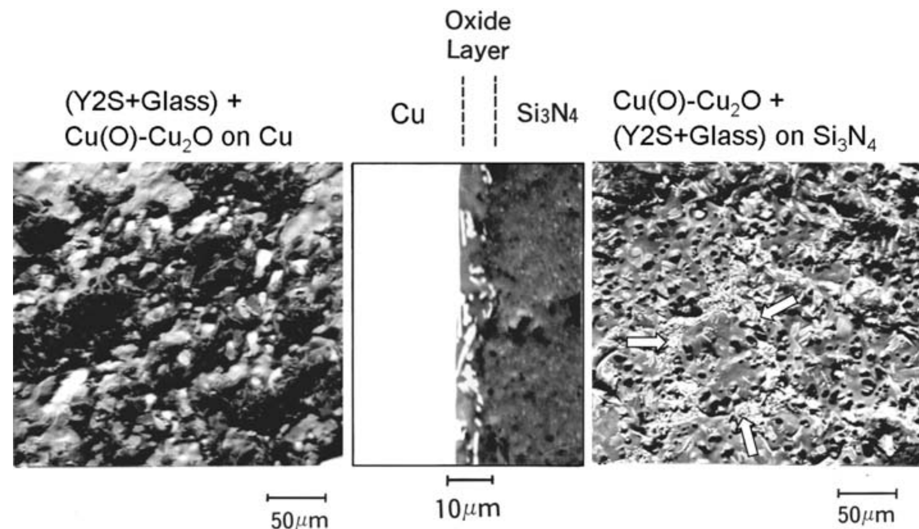

Fig. 9 SEM micrographs of cross-sectional and peeled-off surfaces of the directly bonded Si_3N_4/Cu. Polygonal-network-shaped Cu(O) + Cu_2O shown with *white arrows* in the *right panel* from the recrystallized Cu grain boundary wetted and reacted with the glassy phase on Si_3N_4

Y2S or cristobalite. It is very interesting that polygonal Cu(O) + Cu_2O patterns form on the Si_3N_4 surface and the polygon corresponds to the grain boundary of recrystallized Cu. Partial bonding with glass and local plastic deformation of Cu(O) and Cu_2O may relax residual stress caused by the thermal expansion mismatch between Cu and Si_3N_4. On the Cu surface shown in the left panel of Fig. 9, silicate glass and Y2S surrounded by Cu(O) and Cu_2O polygons appeared as a transferred block. The Si_3N_4 substrate may have been fractured transferring to the Cu side with a decrease in its mechanical strength caused by the high-temperature oxidation.

Mechanism of bonding of Cu to oxidized Si_3N_4

The characteristics of Cu directly bonded to oxidized Si_3N_4 in all regions are summarized in Table 1 from the viewpoints of the oxide layer, bonding strength and the peeled-off surface stated in "Surface morphology and phases in oxidized Si_3N_4", "Shear strength of directly bonded Si_3N_4/Cu", and "Interface structures of bonded Si_3N_4/Cu" sections. The wetting phenomena and the direct reaction of molten Cu and Cu(O) on silicate glass are the origin of Cu/Oxide layer/Si_3N_4 bonding. It is necessary to reconsider the mechanism of bonding between Cu and silicate glass.

When a tough-pitch copper was kept at 1075–1080 °C in the liquid Cu + Cu(O) region of the Cu–O phase diagram, small Cu_2O balls solidified along the grain boundary of recrystallized copper, as shown in Fig. 10. Molten Cu + Cu(O) was supplied mainly from the grain boundary of Cu and wetted the silicate glass well, followed by bonding through the reaction with silicate glass to form a compound at their interface. Below 1065 °C, liquid Cu changed to Cu_2O through the following eutectic reaction:

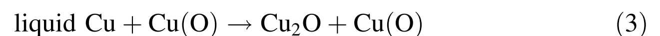

$$\text{liquid Cu} + \text{Cu(O)} \rightarrow Cu_2O + \text{Cu(O)} \quad (3)$$

The other oxide phases such as CuO, Cu_3O_2, $CuAlO_2$, or $CuAl_2O_4$ have not been detected in the polygonal-shaped bonded region. The reasons were first total oxygen content was limited to 0.02–0.05 wt% in solution as Cu(O), and second the temperature for DBC was lower than 1080 °C where $CuAlO_2$ never formed which was studied by in situ high temperature XRD in the author's group [12]. The bonding reaction may be governed by the phase relation at bonding temperatures constructed by Cu_2O or Cu and components of the oxidation products on Si_3N_4, such as silicate glass and some oxides, and a reaction that lowers the total free energy of the system occurs, for example, the formation of a pseudo-solid solution. The further identification of detailed complex phases in the oxidation products

Table 1 Summary of oxidized Si_3N_4, strengths of DBC, and peeled-off surface

Oxidation temp.	Characteristics of the oxide layer on Si_3N_4	Strength of Si_3N_4/Cu joint by DBC	Wetting of molten Cu + Cu_2O appeared in peeled-off surface
Region I (1240–1300 °C)	Y2S (110) parallel to substrate with small amount of silicate glass	Weaker bond 0–20 MPa	Not good → Polygonal pattened Cu(O) + Cu_2O on Si_3N_4
Region II (1300–1350 °C)	Large amount of silicate glass with randomly distributed Y2S	Strong bond ~100 MPa	Good → Silicate glass + Y2S transferred to Cu side
Region III (1350–1415 °C)	α-Cristobalite with orientated Y2S and silicate glass	Weaker or not bonded	–

Fig. 10 Small Cu_2O balls solidified along the grain boundary of recrystallized copper without bonding. After tough-pitch copper was kept in the liquid Cu + Cu(O) area of the Cu–O phase diagram, liquid Cu changed to Cu_2O through a hypo-eutectic reaction. Molten Cu + Cu(O) changed to Cu_2O + Cu(O) below 1065 °C following the eutectic reaction

and wetting/spreading experiments on molten Cu + Cu(O) on the oxides are necessary to explain the bonding mechanism.

Conclusions

The direct bonding of copper to Si_3N_4 having a thermal conductivity $K = 20$ W/m K was successfully achieved through the wetting of molten Cu + Cu(O) to oxidation products on a Si_3N_4 substrate, which were characterized as Y2S and silicate glass based on additives and impurity atoms in Si_3N_4 that diffused out through grain boundaries. The bonding strength of Cu/Si_3N_4 depends on the amount or layer thickness of silicate glass. High bond strength of 90–100 MPa were obtained using a large amount of silicate glass with randomly distributed Y2S, whereas low bond strength were obtained using the Y2S preferred orientation (110) parallel to the Si_3N_4/oxide interface within a small amount of silicate glass. Summarizing the element distributions around the interface, the morphologies of the peeled-off surface and the glass amount dependence of bond strength, it is concluded that the direct reaction or solution between glassy oxide phase and molten Cu + Cu_2O from the Cu grain boundary is the origin of bonding and that the localized bonding state of Cu(O) + Cu_2O acts as a residual stress relaxer. Wetting and spreading experiments on molten Cu + Cu(O) on oxides are required to elucidate the bonding mechanism on the atomic scale.

Acknowledgements The author is indebted to Toshiba Corporation for supplying silicon nitride specimens and for assisting in the analysis of the oxidation products.

References

1. Burgess JF, Neugebauer CA, Flanagan GT (1975) J Electrochem Soc 122:688
2. Mellul S, Chevalier J-P (1991) Philos Mag 64:561
3. Kim ST, Kim CH (1992) J Mater Sci 27:2061. doi:10.1007/BF01117918
4. Yi S, Trumble KP, Gaskell DR (1999) Acta Mater 47:3221
5. Schulz-Harder J (2003) Microelectron Reliab 43:359
6. Tanaka S-I, Nishida K, Ochiai T (1983) In: Proceedings of the international symposium on ceramic components for engine, Hakone, Japan, p 249
7. Kim ST, Kim CH, Park JY, Son YB, Kim KY (1990) J Mater Sci 25:5185. doi:10.1007/BF00580149
8. Singhal SC (1976) J Mater Sci 11:500. doi:10.1007/BF00540931
9. Hasegawa Y, Tanaka H, Tsutsumi M, Suzuki H (1980) Yogyo-Kyokai-Shi 88:292
10. Lange FF, Singhal SC, Kuznicki RC (1977) J Am Ceram Soc 60:249
11. Kiehle AJ, Heung LK, Gielisse PJ, Rockett TJ (1975) J Am Ceram Soc 58:17
12. Fujimura T, Tanaka S-I (1998) Acta Mater 46:3057